Int. J. Econ. Environ. Geol. Vol. 13 (2) 27-34, 2022
Journal home page: www.econ-environ-geol.org

Open Access
ISSN: 2223-957X

Clay-Iron Nanocomposite for the Removal of Sulfur as Toxic Pollutant from Fuel by Catalytic Oxidative Desulfurization

Haris Ahmed[1]*, Erum Zahir[1], Muhammad R. Ibad[2], Muhammad A. Asghar[3]

[1]Department of Chemistry, University of Karachi, Karachi 75270, Pakistan
[2]Department of Chemistry, NED University of Engineering & Technology, Karachi, Pakistan.
[3]PCSIR Laboratories Complex, Karachi, Pakistan.

* Email: haris_ahmed90@live.com

Abstract: The current environmental pollution has great impact on climate change and the present study was aimed at removal of sulfur as a pollutant for environment on combustion of kerosene fuel using clay, namely attapulgite and magnetic iron (ATP)-Fe_3O_4 nanocomposite. To lower the toxic sulfur and to enhance the property of reduced sulfur fuel specifically the electrical conductivity (EC) was also improved by the addition of quality improver additives. The (ATP)-Fe_3O_4 nanocomposite was synthesized by co-precipitation method and the structure, and morphology were evaluated using scanning electron microscopy (SEM), and fourier transform infrared spectroscopy (FT-IR). The average size of Fe-NPs which helps in the oxidative desulfurization was found to be <100 nm, and the toxic sulfur content in fuel was reduced up to 71% from its original using 05mg/mL of nanocomposite at 150°C for 30 min along with CH_3COOH and H_2O_2 proceed with water washing. The EC of the oxidative desulfurized (ODS) fuel was enhanced by the addition of (0.5, 0.7 and 1.0ppm) STADIS 450 additive as compared to MEROX kerosene fuel (untreated). The ODS kerosene showed greater stability of EC over MEROX kerosene.

Keywords: Magnetic nanoparticles, attapulgite-iron oxide nano-composite, oxidative desulfurization, electrical conductivity, kerosene.

Introduction

Sulfur is a major source of air pollution upon combustion of fuel. Ultra-deep desulfurization has gained interest by scientists due to environmental concern and reducing the limit of sulfur up to 100 ppm or less (Ali et al., 2006, Kulkarni and Afonso, 2010). In refineries, the sulfur containing compounds are removed by conventional method such as hydro desulfurization (Srivastava, 2012).

Activated carbon and activated clays are widely used for the removal of organic contaminants due to porous nature, large surface area and the net negative charge on their structure (Juang et al., 1997). Activated clay helps in increasing the catalytic reactions. Attapulgite is a natural fibrous clay mineral hydrated crystalline magnesium and aluminum silicate with great adsorptive properties. (Khorami and Nadeau, 1986). The clay is formed by alteration of montmorollonite clay, and is used for different industrial and medicinal purpose. Attapulgite clay also has the same properties as other clays but different in structure (da Silva et al., 2022). They are needle shaped silicates which are different in length and range from 20 nm to several hundred nanometers (Liu wt al., 2008, Ruiz-Hitzky et al., 2011). The unique morphology of ATP increases its applications such as catalyst support and environmental adsorbent.

Nanoparticles (NPs) are the materials which differ in properties from their bulk and size <100 nm. NPs are naturally occurring materials, as well as can be synthesized. Metallic NPs are widely used in different medical and industrial fields (Iqbal et al., 2012). Magnetite NPs are ferromagnetic that contain both Fe (II) and Fe (III). Super paramagnetic NPs are widely used in applications such as ferro fluids, color imaging, magnetic resonance imaging and in removal of contaminants from aqueous and non-aqueous medium (Oh and Park, 2011, Rumenapp et. al., 2012, Feng, et al., 2019, Yao et al., 2021).

Recently, oxidative desulfurization (ODS) has gained much attention for deep desulfurization of fuel to reduce the toxic sulfur which causes atmospheric pollution upon combustion (Haghighi and Gooneh-Farahani, 2020). Usually, hydrogen peroxide (H_2O_2) is the most common oxidant and used with catalysts such as acetic acid, silicates and solid bases, due to environmental friendliness (Akhmadova et al., 2018). Sulfur containing compounds in fuel is oxidized by H_2O_2 under mild conditions and can be converted to sulfoxides and sulfones which can be separated from oil by distillation, solvent extraction or adsorption (Hulea et al., 2001). In addition, the use of H_2O_2 for ODS is efficient and cost effective (Neumann and Levin-Elad, 1997, Murata et al., 2004, Bokare and Choi, 2016).

In addition, the main component of jet fuel is kerosene, and it is widely used in commercial and fighter jet planes (Rahmes et al., 2009). Naturally, the jet fuel has very low electrical conductivity (EC) which is less than 10 pS/m (CU). The electrostatic charges accumulated during high speed pumping of fuel by

microfiltration, which could be very dangerous (Dacre and Hethrington, 1998). The dissipation of the accumulated charge can reduce the risk of fire and to dissipate these charges the electrical conductivity of fuel is increased (Nabours, 2004). Recently, the STADIS 450 an electrical conductivity improver is used for the increase in electrical conductivity (Dacre and Hetherington, 1998). The STADIS 450 shows different response in fuel from different crude source when doped with the same concentration (Dacre and Hethrington, 1994).

The EC in jet fuels is very sensitive to low concentration of polar compounds. The other additives also influence the EC of fuel. Researchers found that the thermal stability additive (TSA) '+100' has a significant effect on EC response (Taylor et al., 2002). The use of other additives is also part of jet fuel and known as corrosion inhibitor (CI) i.e. DCI-4A and fuel system icing inhibitor (FSII). Chemically corrosion inhibitor is a dimer of linoleic acid and is used to reduce tear in metallic roller bearings in fuel pump and to reduce corrosion in fuel system (Black et al., 1988). The use of FSII (fuel system icing inhibitor) in jet fuels acts as an anti-freezing agent that does not allow the formation of ice crystals which are present in the form of dissolved water (Vozka and Kilaz, 2020).

In this work, the synthesized magnetic NPs were combined with ATP *via* co-precipitation method and were used to desulfurize the jet fuel by catalytic oxidation under varying conditions. In addition, the effect of electrical conductivity additive in different dosages in normal Merox fuel and in ODS fuel was investigated.

Materials and Methods

All chemicals used were of analytical grade hydrogen peroxide (H_2O_2) (30wt %), ferric chloride ($FeCl_3.6H_2O$), calcium sulfate ($CaSO_4$) were obtained from BDH-UK, glacial acetic acid (CH_3COOH) (99% pure), hydrochloric acid (HCl), Ferrous sulfate ($FeSO_4.2H_2O$) were obtained from Sigma Aldrich, n-hexane obtained from Fischer Chemicals, deionized water of conductivity <1.0 µS/cm was used, Sodium hydroxide (NaOH) was purchased from Lab chem. Attapulgite clay (ATP) was obtained from a local supplier, Mylar film was provided by Tanaka Scientific. Kerosene, Stadis-450 (STD-450), DCI-4A, FSII, PLUS 100 were obtained from Innospec by a local supplier. The measurement of EC in fuel was done by electrical conductivity meter (Make: emcee Model: 1152). The magnetic nanoparticles (Fe-NPs) were synthesized using the method reported by Kalantari et al. (2014).

Syntheis of Magnetic Iron Nanoparticles and Nanocomposite

In brief, $FeCl_3.H_2O$ and $FeSO_4.2H_2O$ in a ratio of 2:1 were dissolved in 400 mL water. An aliquot of 100 mL NaOH (5 mol L^{-1}) was added drop wise to the solution under stirring at 80°C. The solution turned to black precipitate (Red'ko and Suprun, 2018). The obtained particles were washed using deionized water (DI-H_2O) which were magnetically separated and then dried under normal atmospheric conditions. The powdered attapulgite clay was passed through a sieve of 200µm mesh size which is subjected to acid treatment. In brief, an amount of 15 g clay was treated with 100 mL of HCl (1 M) and refluxed for 2h under constant magnetic stirring (Boudriche et al., 2011). The clay was washed with DI-H_2O till neutral pH and then dried in an oven at 110°C for 4h and stored in desiccator till further use. The clay composite with Fe-NPs was synthesized by adding an equal amount of dried activated clay and Fe-NPs in 100 mL of deionized water. The solution was stirred for 1h at 70°C, filtered and then dried at room temperature for 4h.

The obtained nanocomposite was characterized using different electro-analytical techniques. A Fourier transform infrared (FT-IR) instrument (Shimadzu IR prestige-21, Japan) was used to determine the formation of metallic bond in nanoparticles using KBr method. The morphology of acid treated clay, Fe-NPs and ATP-Fe nanocomposite were studied using scanning electron microscope (Model # JSM-6380A, JEOL, Japan).

Oxidative Desulfurization of Fuel

In Oxidative desulfurization (ODS) of fuel 0.5 g of ATP-Fe nano-composite was added to 100 mL of kerosene (Dehkordi et al., 2009). Five mL of H_2O_2 and 10 mL of CH_3COOH were added to the same flask which was then placed on a heating mantle and heated at 150°C for half an hour. The organic layer was washed three times with deionized water containing anhydrous calcium sulfate ($CaSO_4$). The ODS of kerosene was evaluated for sulfur content using X-ray fluorescence (Model: RX-XSH). Percent removal was calculated by using following formula.

$$\text{Sulfur removal in percent} = [(S_{initial} - S_{final})/ S_{[initial]}]*100$$

Neat kerosene with electrical conductivity (EC < 10 pS/m) was used, 0.5, 0.7, 1.0 ppm of electrical conductivity improver STADIS 450 was added. The same concentrations of additive were also added to ODS kerosene fuel. Further studies were made with the addition of 20 ppm of corrosion inhibitor DCI-4A, 256 ppm of thermal stability additive +100 and 0.12 vol. % of icing inhibitor additive FSII was added to the same solution. All the samples were performed in triplicate. Each sample was checked after every 3hrs to 24h then up to 3days with 24h interval. EC was noted for each sample and plotted against incubation time. All samples were stored in amber glass bottles. The effect of contact time, amount of adsorbent and temperature were also studied. The synthesis of Fe-NPs was confirmed by the color change phenomenon from orange to brown and

then black precipitate. This color change phenomena was also confirmed by Kim et al. (2017).

The type of adsorbent was selected for maximum removal of sulfur under similar conditions like time temperature and amount. 0.5g of each adsorbent per 100 mL of oil was used for desulfurization at 150°C for 30 minutes as maximum sulfur removal occurred at this amount of adsorbent. The percent removal of sulfur was performed using Fe NPs, ATC, Fe NPs: ATC (1:1), Fe NPs: ATC (2:1).

The various adsorbent factors such as amount of adsorbent, time and temperature effect were studied to optimize the conditions for the maximum removal of sulfur content. Different amount of nanocomposite such as 0.1, 0.2, 0.3, 0.4, 0.5, 0.6 and 0.7 g were used under similar conditions of temperature 150°C, volume 100mL and time 30min to investigate the effect of adsorbent dosage on the desulfurization process.

In order to optimize the maximum removal at different intervals of time, 0.5g of Fe NPs : ATC (1:1) adsorbent was used with 100 mL of fuel. Removal of sulfur in fuel was evaluated at time 0, 5, 10, 20, 30, 40, 50, and 60 min. To select the optimum temperature for the desulfurization of oil, the process was carried out at different temperatures, such as, 40, 60, 80, 100, 120, 140, 160, 180 °C. Other parameters like amount of adsorbent (0.5g), volume of oil (100mL) and contact time (30min) was kept constant.

Results and Discussion

Characterization of Nano-composite

FT-IR Analysis:

Figure 1a shows the FT-IR spectrum of Fe_3O_4 nanoparticles, the peaks at 569.0 and 414.70 cm^{-1} show the absorbance bands of Fe $^{2+}$-O^{2-} and Fe $^{3+}$-O^{2-} bond in the magnetite, respectively (Takai et al., 2019). The peaks at 1652.9 and 3460.3 cm^{-1} show the existence of H_2O remainder in samples (Jin et al., 2017).

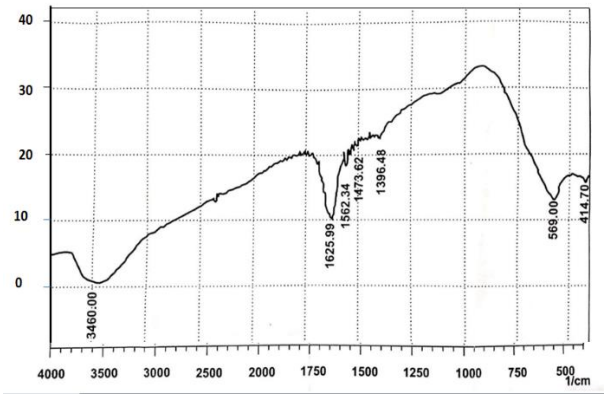

Figure 1b and 1c show the FT-IR spectrum of acid treated ATP and ATP-Fe nanocomposite. The peak at 3400 cm^{-1} shows the characteristic stretching band of –OH groups (Jin et al., 2017). Due to weak absorption peak, the crystallization was considered complete. The peaks at 474.49 and 609.51 cm^{-1} show the absorbance bands of Fe $^{2+}$-O^{2-} and Fe $^{3+}$-O^{2-} bond. The peak at 1033.85 cm^{-1} shows the stretching vibration of Si-O bond (Sebayang et al.,2018).

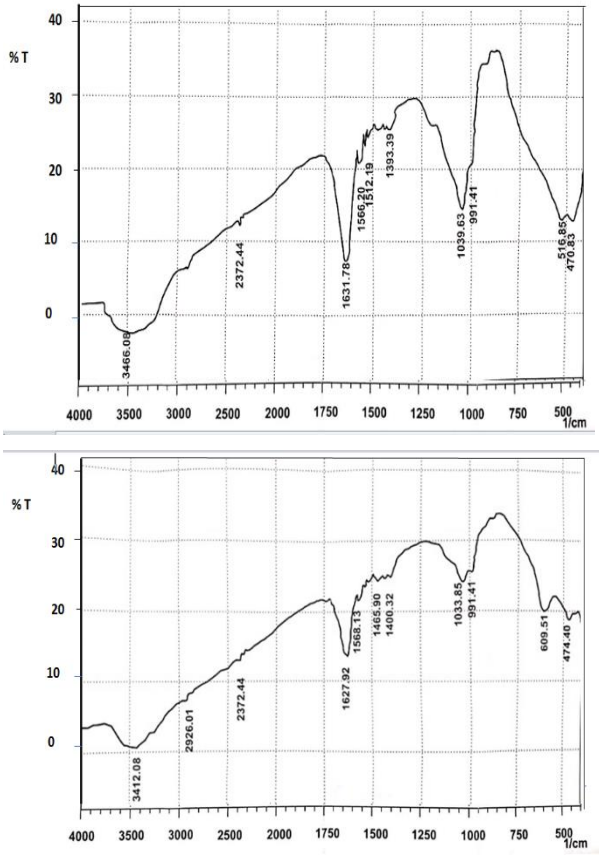

Fig 1.FT-IR spectra of (a) Magnetic Fe-NPs, (b) Acid treated Attapulgite (ATP), (c) ATP-Fe NPs nanocomposite

SEM Analysis

The morphology of acid treated clay, Fe-NPs and ATP-Fe was observed using SEM analysis. Figure 2a shows the uniform and spherical type structure of Fe-NPs with size less than 100 nm at an elevated temperature. Figure 2b shows the fibrous nature of ATP clay remained after acid treatment. Barrios et al. (1995) reported the same observations by treating ATP with strong acid and concluded that the silica could form protective gel during acid activation which keeps its fibrous morphology. The fibrous rod like structure of ATP size of 80 nm has a large surface area and attributed higher surface activity.

The magnetite NPs has completely coated on the rod surface of ATP as revealed by SEM observations. In the surface of ATP-Fe was showing the smooth edges on the surface of ATP which is attributed to the surface change morphology of rod shape ATP (Fig. C).

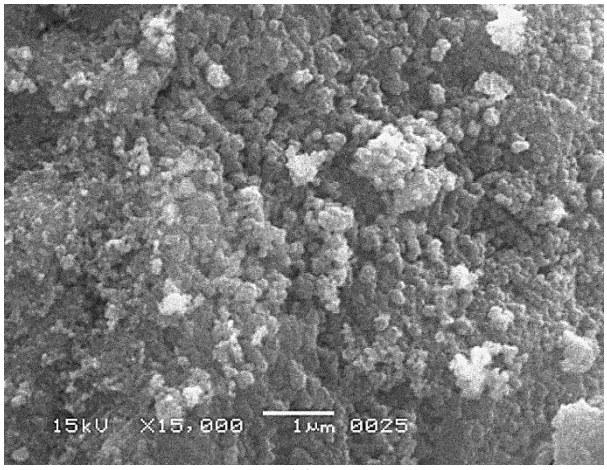

(a)

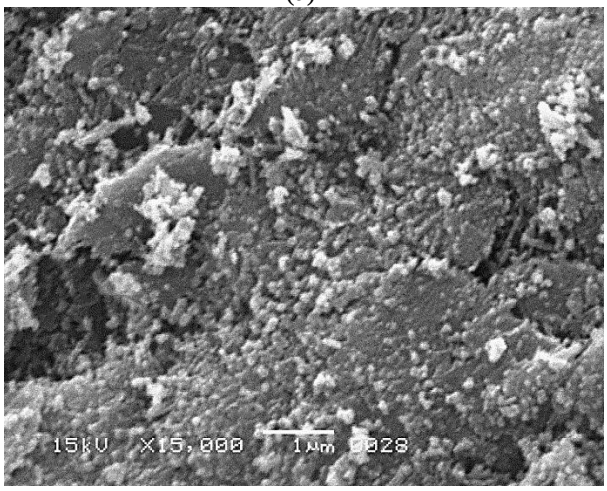

(b)

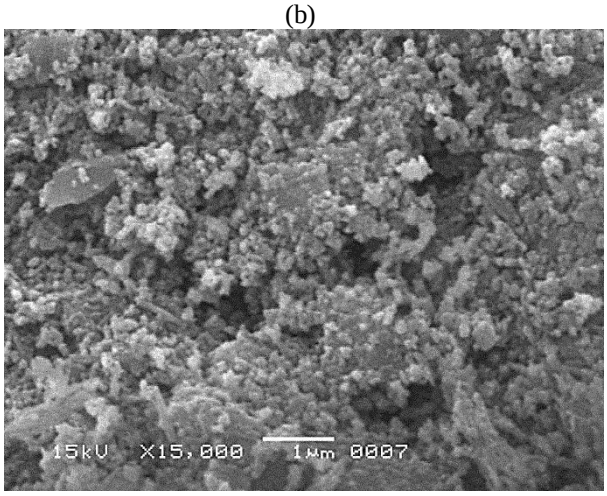

(c)

Fig. 2 SEM image of (a) Fe-NPs, (b) Acid treated ATP clay, (c) ATP-Fe NPs composite

Oxidative Desulfurization of Fuel

About 0.1%, 13% and 51% sulfur removal was found using Fe NPs, ATC and Fe NPs: ATC (2:1) respectively. Whereas, the higher percent removal was found to be 71% which was achieved by Fe NPs: ATC (1:1). The desulfurization property of the nano adsorbents was found in the following order: Fe NPs: ATC (1:1)>Fe NPs: ATC (2:1)>ATC > Fe NPs.

The bare Fe-NPs show the least results in desulfurization as compared to the other nano-adsorbents whereas nanocomposite clay in equal proportion shows the highest percent removal in desulfurization due to its mesoporous activity and surface acidity (Abedinin et al., 2021).

Effect of Adsorbent Amount

Figure 3a shows that the rate of percent removal of sulfur increases with increase in amount of adsorbents and shows the maximum result when 0.5g was used each adsorbent. The percent removal of sulfur with 0.1, 0.2, 0.3, 0.4, 0.5, 0.6 and 0.7g of Fe NPs : ATC (1:1) adsorbent were found to be 17.6, 20.6, 35.2, 52.9, 71.2, 69.4 and 68.5% respectively. The catalyst activity depends upon the acidity and polar aprotic solvents, which is the main reason of maximum sulfur removal at 0.5g of adsorbent used. (Garcia et al., 2008)

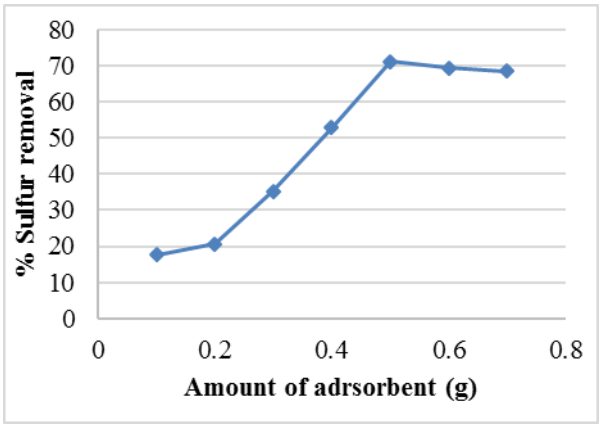

Effect of Contact Time

Figure 3b shows the percent removal of sulfur and the maximum removal was found at time 30 min. The percent removal of the sulfur for the time was found to be 0.06, 14.7, 22.3, 35.3, 71.0, 69.4, 69.9, and 69.8% respectively. The desulfurization rate was slower after 30 min. due to saturation of active sites of the nano-composite and the adsorptive desulfurization has reached to equilibrium. This observation found consistent with literature (Sadare and Daramola, 2019). The time for further desulfurization used was 30min for the optimization of different parameters.

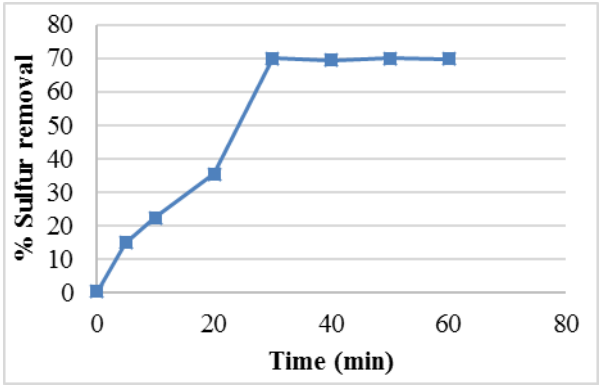

Effect of Temperature

Figure 3c shows that the sulfur removal increases with increased in temperature and the maximum removal was found at 150°C. At higher temperature, the kinetic energy of molecules increases, which increases the removal of sulfur. The commercial clays (K-10 and KSF) as catalyst loaded with Vanadium using H_2O_2 shows the removal of sulfur to 58% and 33% respectively. (de Mello et al., 2018). Furthermore, the diffusion rate in the pores of adsorbent also increase with increase in temperature (Ishaq et al., 2017).

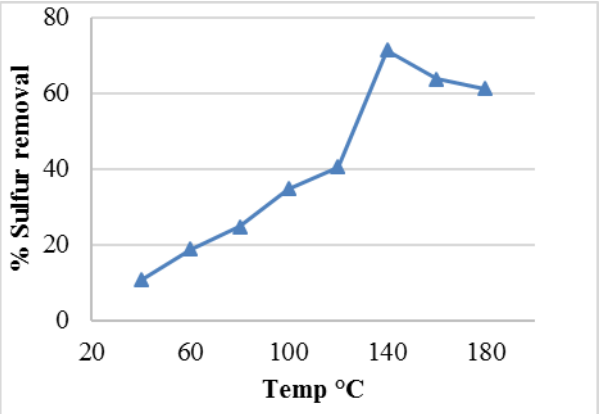

Fig. 3. a) Effect of amount of adsorbent on desulfurization of kerosene fuel, b) Effect of contact time with adsorbent, c) Effect of temperature on desulfurization.

Oxidation of kerosene fuel using nanocomposite clay converts the nonpolar sulfur compounds to polar sulfones and sulfoxides which can be extracted using polar solvents. Hulea et. Al. explained the oxidation of a large number of sulfur compounds in kerosene fraction using H_2O_2 as a solvent (Hulea et al., 2001). It appears that H_2O_2 can be used for the oxidative desulfurization of fuel using nano-composite clay as catalyst. The increase in temperature accelerates the rate of oxidation and H_2O_2 thermal degradation (Zhang et al., 2011). Using other agents for extraction with H_2O_2can also increase the percent removal of sulfur up to > 85%. (Muhammad et. al, 2018). Whereas, in the present study, the sulfur content, was decreased from 0.17 wt/wt % to 0.049 wt/wt % which was 71% removal. The maximum removal was achieved using 0.5g for 30 min at a temperature of 150°C.

Electrical Conductivity in Normal and ODS Fuel

Figure 4 shows that the EC increases by increased dosage of Stadis-450 (STD-450). The limit of EC additive dosage in normal fuel is maximum up to 3 ppm which is set as per standard DEF STAN 91:91. Three sets of different EC additive concentrations 0.5, 0.7, 1.0 ppm were made. The addition of 20 ppm CI in the presence of STD-450 additive does not enhance the EC but to some extent. The addition of FSII to the same solution in another replicate shows the considerable change in the EC. The addition of 100+ additive increases the EC to more than about 100 pS/m. The ODS kerosene (Neat) which is treated by NPs shows the same trend of EC on initial basis.

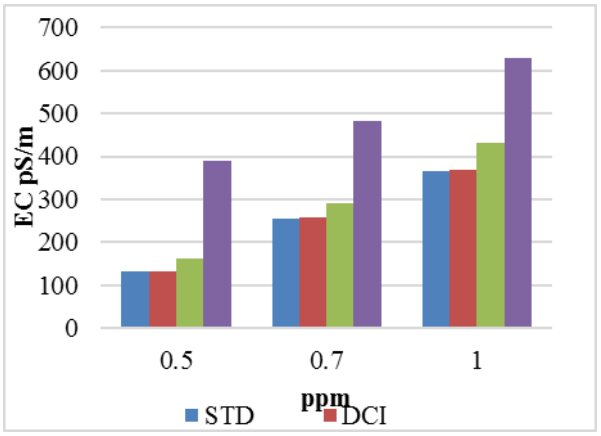

Fig. 4 Effect of different conc. of Stadis-450 with 20ppm DCI-4A and 0.12% FSII and 256ppm plus 100 on Electrical conductivity

The change in EC with respect to time 0, which represents the addition of only STD-450 in ranges of 0.5, 0.7, 1.0 ppm, respectively (Fig. 5). With the interval of time, the EC decreased. However, in low concentration steep decline was observed, which is further increased with respect to time. Three different concentrations of STD-450 i.e. 0.5ppm, 0.7ppm and 1.0ppm doped with the addition of CI, FSII and 256ppm +100. The result shows the similar decline trend in EC with time. However, the ODS fuel shows that the removal of contaminants from the fuel results in stable EC for about 72h (Fig. 5).

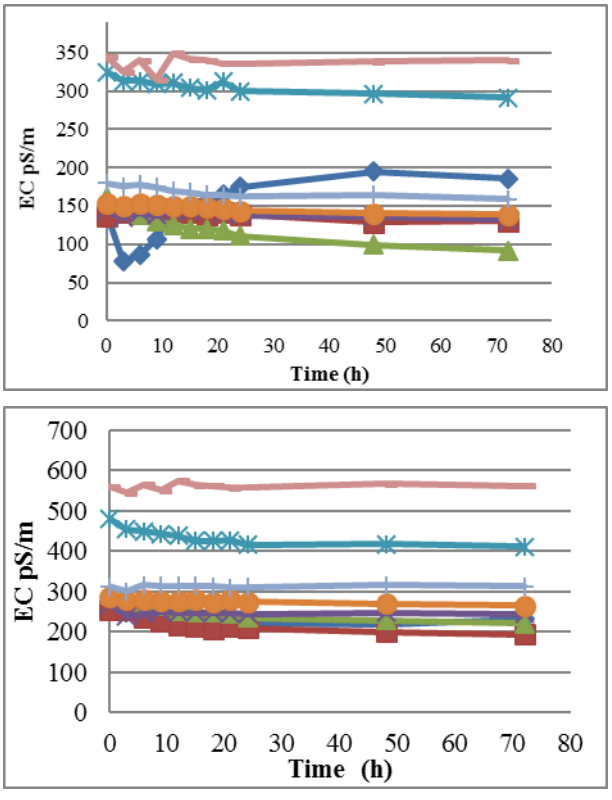

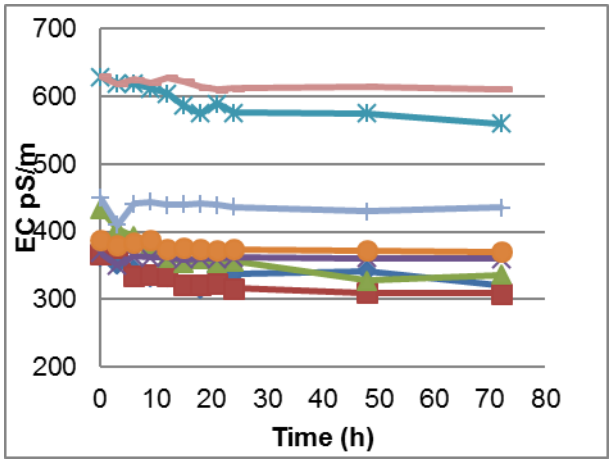

Fig. 5 Effect of different additive DCI-4A, FSII, plus 100 with (a) 0.5ppm, (b) 0.7ppm and (c) 1.0ppm STD-450 in kerosene and ODS kerosene with time.

Conclusion

According to present research, it has been noted that the ATP-Fe nanocomposite worked as an effective catalyst in the removal of sulfur from the kerosene *via* oxidative desulfurization process which helps in reduction of atmospheric pollution. The polar nature of sulfones which were produced by the ODS has affinity towards the hydroxylated surface on the ATP-Fe nanocomposite. The magnetic nature of Fe NPs aids in the removal of polar components formed by oxidative desulfurization. It has been noted that the ATP-Fe nano-composite serve as an effective catalyst for the oxidative desulfurization as well a good adsorbent for the removal of contaminants formed by MEROX process. The highly polar sulfone compounds were adsorbed on the hydroxylated surface on the ATP-Fe nano-composite. The advantage of this process required mild operating conditions.

The effect on conductivity depends upon the STADIS-450 and the type of kerosene. The salt content present in the MEROX based kerosene causes the conductivity of the STADIS solution to fall and then again increases for low concentration of STD-450. However, it continuously declined for other high concentrations of STD-450. The Kerosene doped with STADIS-450 and with other additives like corrosion inhibitor, FSII and thermal stability additive (TSA) i.e. +100 show some response. Lubricity improver DCI-4A has a minor effect on conductivity. However, the FSII and TSA increase the conductivity to some drastic level. The time effect shows that the conductivity trend falls gradually. The ODS kerosene using ATP-Fe nanocomposite catalyst lowers the contaminant due to its polar and magnetic nature which leads to a stable conductivity effect in the kerosene and shows minimum decline in EC with time. The ODS kerosene generates the lesser pollutants in the atmosphere upon combustion.

References

Abedini, F., Allahyari, S., Rahemi, N. (2021). Oxidative desulfurization of dibenzothiophene and simultaneous adsorption of products on BiOBr-C3N4/MCM-41 visible-light-driven core-shell nano photocatalyst.*App. Surface Science*, 151086.

Akhmadova, K., Makhmudova, L. S., Khadisova, Z. T., Abdulmezhidova, Z., Krasnikov, P., IdrisovaE.,Magomadova, M. K. (2018). Oxidative Methods of Desulfurization Of Diesel Fuels. Results, Problems,Perspective. In Proceedings of the International Symposium Engr. and Earth Sci.: App. and FundamentalResearch 422-431 pages.

Ali, M. F., Al-Malki, A., El-Ali,B., Martinie, G, Siddiqui, M. N. (2006) .Deep desulphurization of gasoline and diesel fuels using non-hydrogen consuming techniques.*Fuel.* **85**(10-11), 1354-1363.

Barrios, M. S., González,L. F., Rodriguez, M. V., Pozas,J. M. (1995). Acid activation of a palygorskite with HCl Development of physico-chemical, textural and surface properties.*App. Clay Sci.***10**(3), 247-258.

Black, B. H., Wechter, M. A., Hardy, D. R. (1988). Determination of corrosion inhibitor/lubricity enhancer additives in jet fuels by size-exclusion chromatography.*J. of Chrom. A.* **437**, 203-210.

Bradley, W. (1940). The structural scheme of attapulgite. *American Mineralogist: Journal of Earth and Planetary Materials, **25*(6),** 405-410.

Bokare, A. D., Choi, W. (2016). Bicarbonate-induced activation of H_2O_2 for metal-free oxidative desulfurization. *J. of Haz.Mat.***304**, 313-319.

Boudriche, L., Calvet, R., Hamdi, B., Balard, H. (2011). Effect of acid treatment on surface properties evolution of attapulgite clay: an application of inverse gas chromatography. *Colloids and Surf. A: Physicochemical and Engineering Aspects.* **392**(1), 45-54.

da Silva, T. F., de Souza, G. P. M., de Melo Morgado, G. F., Albers, A. P. F., Quinteiro, E., & Passador, F. R. (2022). Influence of surface modification of attapulgite (ATP) with aminosilane (3-aminopropyl) triethoxysilane for the preparation of LLDPE/ATP nanocomposites. *Journal of Polymer Research, **29*(3)**, 1-13.

Dacre, B., Hetherington, J. I., (1994). Behavior of conductivity improvers in jet fuel. In Abstract Volume, 5th International conference onstability and handling of liquid fuels, Rotterdam, The Netherlands, 43.

Dacre, B., Hetherington, J. I. (1998). The effects of contaminants on the behaviour of conductivity improvers in hydrocarbons. *J. of electrostatics.* **45**(1),53-68.

de Mello, M. I., Sobrinho,E. V., Teixeira da Silva, V., Pergher, S. B. (2018). Vanadium incorporation in montmorillonite clays for oxidative diesel desulfurization. *Ind. and Engr. Chem. Research.* **57**(46), 15663-15669.

Dehkordi, A. M., Sobati, M. A., Nazem, M. A. (2009). Oxidative desulfurization of non-hydrotreated kerosene using hydrogen peroxide and acetic acid. *Chinese J. of Chem. Engineering* .**17**(5), 869-874.

Feng, Z., Zhu, Y., Zhou, Q., Wu, Y., Wu, T. (2019). Magnetic WO_3/Fe_3O_4 as catalyst for deep oxidative desulfurization of model oil.*Materials Science and Engineering: B* **240**,85-91.

García-Gutiérrez, J. L., Fuentes, G. A., Hernandez-Teran, M. E., Garcia,P., Murrieta-Guevara,F. Jiménez-Cruz, F. (2008). Ultra-deep oxidative desulfurization of diesel fuel by the Mo/Al_2O_3-H_2O_2 system: The effect of system parameters on catalytic activity. *App. Cat. A: General* **334**(1-2), 366-373.

Haghighi, M., Gooneh-Farahani, S. (2020). Insights to the oxidative desulfurization process of fossil fuels over organic and inorganic heterogeneous catalysts: advantages and issues. *Environmental Science and Pollution Research, **27*****(32),*** 39923-39945.

Hulea, V., Fajula, F., Bousquet, J. (2001). Mild oxidation with H_2O_2 over Ti-containing molecular sieves—a very efficient method for removing aromatic sulfur compounds from fuels. *J. of cat.***198**(2), 179-186.

Iqbal, P., Preece,J. A., Mendes, P. M. (2012). Nanotechnology: The "Top - Down" and "Bottom - Up"Approaches.Supramolecular chemistry: from molecules to nanomaterials. John Wiley & Sons.

Ishaq, M., Sultan, S., Ahmad, I., Ullah, H., Yaseen, M., Amir, A. (2017). Adsorptive desulfurization of model oil using untreated, acid activated and magnetite nanoparticle loaded bentonite as adsorbent. *Journal of Saudi Chemical Society, **21***(2), 143-151.

Jin, Z., Zhong, M., Wang, F., Dong, Y., Lei, Z., Wang, Q., Su, B. (2017). Enhanced magnetic and electrochemical properties of one-step synthesized PANI-Fe_3O_4 composite nanomaterial by a novel green solvothermal method. *J. of Alloys and Comp.***695,** 1807-1812.

Juang, R., Wu, F., Tseng, R. (1997). The ability of activated clay for the adsorption of dyes from aqueous solutions.*Env. Tech.***18**(5), 525-531.

Khorami, J., Nadeau, D. (1986). Physicochemical characterization of asbestos and attapulgite mineral fibers before and after treatment with phosphorus oxychloride. *Thermochimica acta, **108,*** 279-287.

Kalantari, K., Ahmad, M. B., Shameli, K., Hussein, M. Z. B., Khandanlou, R., Khanehzaei,H. (2014). Size-controlled synthesis of Fe_3O_4 magnetic nanoparticles in the layers of montmorillonite.*J. of Nanomaterials.* **2014**, e739485.

Kim, K. T., Yoon,S. A., Ahn, J., Choi, Y., Lee,M. H., Jung, J. H. Park, J. (2017). Synthesis of fluorescent naphthalimide-functionalized Fe_3O_4 nanoparticles and their application for the selective detection of Zn^{2+} present in contaminated soil. *Sensors and Actuators B: Chemical.* **243**,1034-1041.

Kulkarni, P. S., Afonso,C. A. (2010). Deep desulfurization of diesel fuel using ionic liquids: current status and future challenges. *Green Chem.***12**(7), 1139-1149.

Liu, Y., Liu,P., Su,Z., Li,F., Wen, F. (2008). Attapulgite–Fe3O4 magnetic nanoparticles via co-precipitation technique. *App. Surface Sci.***255**(5), 2020-2025.

Muhammad, Y., Shoukat,A., Rahman, A. U., Rashid,H. U., Ahmad, W. (2018). Oxidative desulfurization of dibenzothiophene over Fe promoted $Co–Mo/Al_2O_3$ and $Ni–Mo/Al_2O_3$ catalysts using hydrogen peroxide and formic acid as oxidants.*Chinese J. of Chemical Engineering* **26**(3), 593-600.

Murata, S., Murata, K., Kidena, K., Nomura, M. (2004). A novel oxidative desulfurization system for diesel fuels with molecular oxygen in the presence of cobalt catalysts and aldehydes. *Energy and fuels.* **18**(1), 116-121.

Nabours, R. E. (2004). Static discharge hazard during refueling at retail gasoline stations. *IEEE Transactions on Industry Applications, **40***(4), 1003-1005

Neumann, R., Levin-Elad,M. (1997). Metal oxide (TiO_2, MoO_3, WO_3) substituted silicate xerogels as catalysts for the oxidation of hydrocarbons with hydrogen peroxide.*J. of Cat.* **166**(2), 206-217.

Oh, J. K., Park,J. M. (2011). Iron oxide-based superparamagnetic polymeric nanomaterials: design, preparation, and biomedical application. *Prog. in polymer Sci.***36**(1), 168-189.

Rahmes, T., Kinder,J., Crenfeldt, G., LeDuc, G., Abe, Y., McCall, M., Henry,T., Zombanakis, G., Lambert,D., Lewis, C., (2009). Sustainable bio-derived synthetic paraffinic kerosene (Bio-SPK) jet fuel flights and engine tests program results.*9th AIAA aviation technology, integration, and operations conference (ATIO) and aircraft noise and emissions reduction symposium* (ANERS).

Red'ko, Y. V., Suprun, N. (2018). XRD and SEM analysis of iron oxide nanoparticles formation in polyamide textile material. *Fibres Text* **3**, 63-67.

Ruiz-Hitzky, E., Aranda,P., Álvarez,A., Santarén, J., Esteban-Cubillo, A. (2011). Advanced materials and new applications of sepiolite and palygorskite. *Developments in Clay Science, Elsevier*. **3,**393-452.

Rümenapp, C., Gleich,B., Haase, A.(2012). Magnetic nanoparticles in magnetic resonance imaging and diagnostics.*Pharmaceutical Research* **29**(5), 1165-1179.

Sadare, O. O., Daramola, M. O. (2019). Adsorptive removal of dibenzothiophene from petroleum distillates using pomegranate leaf (Punica granatum) powder as a greener adsorbent. *Chemical Engineering Communications, **206***(3), 333-345.

Srivastava, V. C. (2012). An evaluation of desulfurization technologies for sulfur removal from liquid fuels. *Rsc Advances, **2*****(3)**, 759-783.

Sebayang, P., Kurniawan, C., Aryanto,D., Setiadi, E. A., Tamba, K., Sudiro, T., (2018). Preparation of Fe_3O_4/bentonite nanocomposite from natural iron sand by co-precipitation method for adsorbents materials. *IOP Conference Series: Materials Science and Engineering*, IOP Publishing.

Takai, Z. I., Mustafa, M. K., Asman, S.,Sekak, K. A. (2019). Preparation and characterization of magnetite (Fe_3O_4) nanoparticles by sol-gel method.*Int. J. Nanoelectron. Mater***.12**, 37-46.

Taylor, S. E., Forester, D. R., Malik,B. B. (2002). Jet fuel thermal stability additives-Electrical conductivity and interactions with static dissipator additive. *SAE Transactions*, 560-564.

Vozka, P., Kilaz, G. (2020). Determination of jet fuel system icing inhibitor by GC× GC-FID. *Talanta* **218,** 121146.

Yao, L., Esmaeili, H., Haghani,M., Roco-Videla, and A. (2021). Activated Carbon/Bentonite/Fe_3O_4 as Novel Nanobiocomposite for High Removal of Cr (VI) Ions.*Chem. Engr and Tech.***44**(10), 1908-1918.

Zhang, J., Wang, A., Li,X., Ma, X. (2011). Oxidative desulfurization of dibenzothiophene and diesel over [Bmim] 3PMo12O40.*J. of cat.***279**(2), 269-275.